Longitudinal spin polarization in multiphoton Bethe-Heitler pair production

Tim-Oliver Müller[1,2] and Carsten Müller[1,3]
[1]*Max-Planck-Institut für Kernphysik, Saupfercheckweg 1, D-69117 Heidelberg, Germany*
[2]*Physik Department, Technische Universität München, D-85747 Garching, Germany*
[3]*Institut für Theoretische Physik, Heinrich-Heine-Universität Düsseldorf, D-40225 Düsseldorf, Germany*
(Received 5 June 2012; published 9 August 2012)

Helicity transfer in electron-positron pair production by a relativistic proton colliding with an intense laser beam of circular polarization is studied. The pairs are produced nonlinearly via absorption of few laser photons. Our approach relies on the laser-dressed description of the leptons by relativistic Volkov states and the spin-projection formalism. We calculate spin-resolved production rates, differential in the energy and emission angle of one of the created leptons. The degree of longitudinal polarization is shown to depend on the number of laser photons involved, even when the total energy and momentum absorbed from the laser field is kept constant.

DOI: 10.1103/PhysRevA.86.022109 PACS number(s): 12.20.Ds, 13.88.+e, 32.80.Wr, 42.55.Vc

I. INTRODUCTION

Since the discovery of electrons with longitudinal spin polarization from nuclear β decay [1], the role of the electronic spin has been investigated in manifold processes. Polarized electron beams may arise, in particular, when electrons interact with photons of definite helicity. Corresponding studies were carried out on photoionization [2], Compton scattering [3], and bremsstrahlung [4,5]. The spin polarization was also studied for the electrons and positrons produced via the Bethe-Heitler effect,

$$Z + \omega_\gamma \to Z + e^+e^-, \tag{1}$$

where a γ photon of energy $\hbar\omega_\gamma > 2mc^2$ decays into an e^+e^- pair in the vicinity of an atomic nucleus of charge number Z [4,5]. We note that reaction (1) is currently utilized for the generation of polarized electron and positron beams [6,7], which are of interest, e.g., for future experiments in high-energy physics.

The photoinduced processes mentioned above possess nonlinear generalizations when the applied photon intensity is very large. Then, multiphoton reactions can take place, where several or even many laser photons participate jointly. Photon intensities this high can be obtained when the photon source is an intense laser field. Nonlinear processes in strong laser fields are being studied intensively both in experiment and theory [8–11]. In particular, the influence of the electron spin on laser-induced processes has been examined theoretically during the last decade with respect to free-electron motion [12,13], two-photon ionization [14,15], high-harmonic generation [16], nonlinear Compton scattering [17], laser-assisted Mott scattering [18,19], and pair production by a high-energy γ photon and a laser field [20,21]. In addition, characteristic differences between fermionic and bosonic particles have been found for pair production in an oscillating electric field [22] and in recent investigations of the Klein paradox [23].

Also the nonlinear Bethe-Heitler process,

$$Z + n\omega_L \to Z + e^+e^-, \tag{2}$$

involving simultaneous absorption of $n > 1$ laser photons of energy $\hbar\omega_L$, has encountered sustained interest in recent years. This interest has been stimulated by the prospect that process (2) may come into experimental reach by combining an intense laser source with a powerful ion accelerator. The setup of colliding laser and nuclear beams effectively enhances the laser field strength and frequency in the projectile frame by the relativistic Doppler effect. For example, when a beam of x-ray photons with $\hbar\omega_L = 5$ keV collides head-on with a counterpropagating proton beam of Lorentz factor $\gamma = 50$, then the Doppler-boosted photon energy in the proton frame is enhanced by a factor $\approx 2\gamma$ and thus closely approaches mc^2. In a similar setup based on ultrarelativistic electrons colliding with an intense optical laser beam, nonlinear pair creation by a high-energy γ photon in a laser field has been observed at the Stanford Linear Accelerator Center (SLAC; Stanford, California, United States) [24].

Different interaction regimes of reaction (2) can be distinguished [25]. They are mainly characterized by the ratio of laser electric field amplitude F_L and laser frequency, which can be combined into a dimensionless parameter $\xi \propto F_L/\omega_L$ [see Eq. (15) below]. When $\xi \ll 1$, the pair production is said to occur in the multiphoton regime; the corresponding production rate shows a power-law dependence of the form $R \sim \xi^{2n}$. In contrast, when $\xi \gg 1$ (but F_L is still undercritical), the rate exhibits a nonperturbative exponential behavior reminiscent of a quantum tunneling process. Therefore, process (2) in this regime is often referred to as tunneling pair production.

Various aspects of the nonlinear Bethe-Heitler process have already been investigated. Total pair-production rates as well as angular and energy distributions of the created particles in the various interaction regimes have been calculated by several authors [26–32]. The influence of bound atomic states [33], of the nuclear recoil [34,35], and of the relative phase in a bichromatic laser field [36] have been analyzed as well. While these calculations always involved a summation over the spins of the produced leptons, spin-resolved calculations have been performed only very recently [37,38]. Both articles considered the tunneling regime. Via a helicity analysis it was found that leptons with the same helicity as the laser photons are emitted in the laboratory frame under slightly larger angles with respect to the nuclear beam than those with opposite helicity [37]. In addition, the internal spin-polarization vector of the electron was shown to be proportional in magnitude to F_L and, to leading order, directed along the electron's transverse momentum component [38]. For pair creation by

a real high-energy photon propagating in a laser field, similar studies based on helicity states and the internal spin vector, respectively, have been carried out [20,21].

In the present paper we perform a spin analysis of the nonlinear Bethe-Heitler process in the multiphoton regime ($\xi \ll 1$). Pair production by absorption of $n = 1,2$, and 3 laser photons of definite helicity is considered. The present study thus complements the previous considerations in [37,38]. Our approach incorporates the spin-projection formalism into the well-established theoretical framework of treating reaction (2) by using relativistic Volkov states [26,27,29–31]. We calculate spin-resolved production rates in both the proton's rest frame and the laboratory frame for various laser parameters. The helicity transfer is evaluated in terms of the degree of longitudinal polarization of one of the created leptons. We demonstrate that our calculations represent a multiphoton generalization of the well-known results on the spin polarization in the linear Bethe-Heitler process (1). Moreover, the degree of longitudinal polarization obtained in the nonlinear Bethe-Heitler process is shown to depend on the photon number n, even under the condition that the total energy $n\hbar\omega_L$ is kept constant.

This paper is organized as follows. In Sec. II we present the theoretical tools used, including the spin formalism of relativistic quantum mechanics and our calculational framework to obtain pair-production rates for each leptonic spin constellation. The results of these calculations for the single-photon case will be presented in Sec. III and for the multiphoton case in Secs. IV and V. The main focus of our discussion will be on the degree of longitudinal polarization of the produced particle beams for different sets of laser parameters. Section VI gives a conclusion of the main results and an outlook on the possibilities for an experimental realization.

II. THEORETICAL FRAMEWORK

This section deals with the theoretical methods that are used to calculate spin-resolved pair-production rates in a circularly polarized laser field and a nuclear field. The produced particles' spin states are taken into account by way of the spin-projection formalism, which is briefly summarized for the reader's convenience in Sec. II A. In Secs. II B and C the spin-dependent matrix elements and production rates for the nonlinear Bethe-Heitler reaction (2) are evaluated. The laser field will be treated as a classical electromagnetic plane wave of definite helicity. The nucleus is described as an external Coulomb field; the nuclear spin degree of freedom is not taken into account.

Throughout this section, atomic units (with $\hbar = m = e = 4\pi\varepsilon_0 = 1$) are used in order to simplify the notation. We apply the metric tensor of flat Minkowskian space-time $\eta^{\mu\nu} = \mathrm{diag}(+,-,-,-)$, so that the scalar product of two four-vectors $a^\mu = (a^0,\boldsymbol{a})$ and $b^\mu = (b^0,\boldsymbol{b})$ is given by $(ab) = \eta_{\mu\nu}a^\mu b^\nu = a^0b^0 - \boldsymbol{ab}$. Furthermore, Feynman's slash notation is used, $\not{a} = (\gamma a)$, where γ^μ are the γ matrices in Dirac representation.

A. Spin formalism

The operator projecting on lepton states associated with a certain spin direction reads [39]

$$\Sigma(s) = \tfrac{1}{2}(\mathbb{1} + \gamma^5 \not{s}). \tag{3}$$

This operator allows decomposing a given spinor in two contributions depending on whether the spin is parallel or antiparallel to a certain direction, defined by the spin four-vector $s^\mu = (s^0,\boldsymbol{s})$. In a particle's rest frame, this spin vector

$$s^\mu = (0,\hat{\boldsymbol{n}}) \tag{4}$$

is strictly spacelike, pointing into a direction of choice given by the unit vector $\hat{\boldsymbol{n}}$. Its scalar product with the momentum four-vector $p^\mu = (E/c,\boldsymbol{p})$, which is given by $(c,0,0,0)$ in the particle's rest frame, therefore obeys the relation

$$(sp) = 0 \tag{5}$$

in any frame of reference. Together with its normalization condition,

$$s^2 = -1\,, \tag{6}$$

a spin vector s^μ can be constructed which is related not to a particle at rest but to a moving particle. To account for the lepton spin, the free spinor wave functions are labeled $u_{p,s}$ for a positive-energy eigenstate (an electron) and $v_{p,s}$ for a negative-energy eigenstate (a positron).

While the theoretical method developed in the next section is applicable to any spin basis, in the subsequent numerical calculations we will focus on the particular spin basis associated with helicity eigenstates. This basis corresponds to the case where the spatial components of the spin vector are parallel (or antiparallel) to the direction of the particle's motion given by $\boldsymbol{p}$. One can easily solve the relations (5) and (6) for s^μ under the assumption that the vector $\boldsymbol{s}$ is parallel or antiparallel to the momentum vector $\boldsymbol{p}$. The solutions are

$$s^0_{\mathrm{R,L}} = \pm\frac{|\boldsymbol{p}|}{c}, \qquad \boldsymbol{s}_{\mathrm{R,L}} = \pm\frac{E}{c^2}\,\hat{\boldsymbol{p}}\,, \tag{7}$$

with the unit vector $\hat{\boldsymbol{p}} = \boldsymbol{p}/|\boldsymbol{p}|$. The corresponding spinor wave functions are eigenstates of the helicity operator with eigenvalues ± 1. Accordingly, the vector s_{R} (s_{L}) is referred to as the spin four-vector of a right-handed (left-handed) particle. The spin basis (7) is distinguished by the property that the helicity can be measured simultaneously with the particle momentum since the corresponding operators commute.

B. Spin-dependent production rates

The nonlinear Bethe-Heitler pair creation of Eq. (2) occurs due to the superposition of the nuclear field and the laser field. It is convenient to perform the calculation of the pair-production rate in the rest frame of the nucleus. In this frame, the nuclear four-potential $A^\mu_N(x)$ consists only of a static scalar component:

$$A^\mu_N = \left(A^0_N,0,0,0\right) \text{ with } A^0_N = \frac{Z}{|\boldsymbol{r}|}\,. \tag{8}$$

The laser field is assumed to be a left circularly polarized laser wave, so that all photons have helicity $+1$. The four-potential of the laser field accordingly reads

$$A^\mu_L(x) = a^\mu_1\cos(kx) + a^\mu_2\sin(kx)\,, \tag{9}$$

where $k^\mu = (1,0,0,1)\,\omega_{\rm nuc}/c$ denotes the wave four-vector, with $\omega_{\rm nuc} = (1+\beta)\gamma\,\omega_L$ being the photon energy in the nuclear rest frame. $\beta = (1-\gamma^{-2})^{1/2}$ denotes the reduced velocity of the proton in the laboratory. The potential is given in radiation gauge so that the vectors $a_1^\mu = (0,a,0,0)$ and $a_2^\mu = (0,0,a,0)$ are strictly spacelike. The laser electric field strength amounts to $F_{L,\rm nuc} = a\omega_{\rm nuc}/c$ in this frame.

Within the standard approach to the problem, the process of nonlinear Bethe-Heitler pair production is considered as a transition from a Volkov state with negative energy to a Volkov state with positive energy induced by the Coulomb field A_N^0 of the nucleus. The corresponding transition amplitude reads

$$S_{p_+s_+,p_-s_-} = \frac{i}{c}\int \overline{\Psi}^{(-)}_{p_-,s_-} \not{A}_N \Psi^{(+)}_{p_+,s_+}\, d^4x. \tag{10}$$

The Volkov states are exact solutions of the Dirac equation in the presence of an external electromagnetic field in the form of a plane wave. As a consequence, the transition amplitude (10) accounts for the interaction of the leptons with the laser field to all orders, this way allowing the treatment of multiphoton processes. The interaction with the nuclear field is treated in the lowest order of perturbation theory.

For a general plane laser wave, the Volkov states can be given as [40]

$$\Psi^{(\pm)}_{p,s}(x) = N_p\left(1 \pm \frac{\not{k}\not{A}_L}{2c(kp)}\right) w_{p,s}\exp\left(\frac{i}{\hbar}\Lambda^{(\pm)}\right), \tag{11}$$

where the upper index denotes the sign of the particle's charge. According to that index, the spinor $w_{p,s}$ is either a free electronic spinor $u_{p,s}$ or a free positronic spinor $v_{p,s}$ [39]. The occurring action is given as

$$\Lambda^{(\pm)} = \pm(px) + \frac{1}{c(kp)}\int^\eta \left[(pA_L) \mp \frac{1}{2c}A_L^2\right] d\tilde{\eta}\,, \tag{12}$$

where $\eta = (kx)$. In these Volkov states, due to the dressing by the laser field, the leptons attain an effective mass

$$m_* = \sqrt{1+\xi^2} \tag{13}$$

and effective momenta

$$q^\mu = p^\mu + \xi^2\frac{c^2}{2(kp)}k^\mu\,. \tag{14}$$

Here,

$$\xi = \frac{1}{c^2}\sqrt{-\overline{A_L^2}} \tag{15}$$

denotes the dimensionless Lorentz invariant intensity parameter mentioned in the Introduction which may be associated to the plane-wave laser field. For the circularly polarized wave of Eq. (9), we have $\xi = a/c^2$. The normalization constant in Eq. (11) is chosen as $N_p = (c/q^0)^{1/2}$.

Including the explicit form of the laser wave (9) into the Volkov states (11), the transition amplitude (10) becomes (see also Eq. (8) in [26])

$$\begin{aligned} S_{p_+s_+,p_-s_-} = {} & \frac{iZ}{\sqrt{q_+^0 q_-^0}}\int\frac{d^4x}{|\boldsymbol{r}|}\,\overline{u}_{p_-,s_-}\left\{\not{\epsilon} - \frac{a^2(\epsilon k)}{2c^2(kp_+)(kp_-)}\not{k}\right. \\ & + \left[\frac{\not{\epsilon}\not{k}\not{a}_1}{2c(kp_+)} - \frac{\not{a}_1\not{k}\not{\epsilon}}{2c(kp_-)}\right]\cos\eta \\ & \left. + \left[\frac{\not{\epsilon}\not{k}\not{a}_2}{2c(kp_+)} - \frac{\not{a}_2\not{k}\not{\epsilon}}{2c(kp_-)}\right]\sin\eta\right\} v_{p_+,s_+} \\ & \times e^{-i\alpha_1\sin\eta + i\alpha_2\cos\eta}e^{i(q_-+q_+)\cdot x}. \end{aligned} \tag{16}$$

Here we introduced the notation $\epsilon^\mu = (1,0,0,0)$, so that $\not{\epsilon} = \gamma^0$, and $\alpha_j = \frac{(a_j p_-)}{c(kp_-)} - \frac{(a_j p_+)}{c(kp_+)}$ for $j = 1,2$. In order to perform the space-time integrations, it is useful to apply the series expansion [41]

$$e^{-i\zeta\sin\eta} = \sum_{n=-\infty}^{\infty} J_n(\zeta)\,e^{-in\eta} \tag{17}$$

to the periodic functions depending on the space-time coordinates in Eq. (16). $J_n(\zeta)$ denotes the nth order Bessel function of the first kind. The transition amplitude can then be written as

$$S_{p_+s_+,p_-s_-} = \frac{iZ}{\sqrt{q_+^0 q_-^0}}\sum_n \mathfrak{M}^{(n)}_{p_+s_+,p_-s_-}\int\frac{d^4x}{|\boldsymbol{r}|}e^{i(q_++q_--nk)x}, \tag{18}$$

with a momentum- and spin-dependent matrix element $\mathfrak{M}^{(n)}_{p_+s_+,p_-s_-}$ that does not depend on any of the space-time coordinates. This matrix element will be dealt with in the next section.

Performing the integration over time in Eq. (18) produces an energy-conserving delta function $\delta(q_+^0 + q_-^0 - nk^0)$. Note that, accordingly, only integer multiples of the photon energy can be absorbed from the radiation field, although we did not take quantization of the laser wave into account in the first place. Consequently, a minimum number of photons n_0 exists that has to be absorbed to overcome the threshold energy for pair production in the proton's rest frame. This minimum number is given by

$$n_0 := \min\{n \in \mathbb{N} : n\omega_{\rm nuc} \geqslant 2m_*c^2\}. \tag{19}$$

Also the spatial integral in Eq. (18) can be taken analytically, producing the Fourier transform of the Coulomb potential. As a result, we obtain

$$S_{p_+s_+,p_-s_-} = \frac{iZ}{\sqrt{q_+^0 q_-^0}}\sum_{n\geqslant n_0}\mathfrak{M}^{(n)}_{p_+s_+,p_-s_-}\frac{4\pi}{\boldsymbol{Q}_n^2}\,2\pi\delta\big(Q_n^0\big), \tag{20}$$

with the four-vector $Q_n^\mu = (Q_n^0, \boldsymbol{Q}_n) = q_-^\mu + q_+^\mu - nk^\mu$ denoting the momentum transfer to the nucleus.

The squared absolute value of the transition amplitude is given by

$$|S_{p_+s_+,p_-s_-}|^2 = \sum_{n\geqslant n_0}\big|S^{(n)}_{p_+s_+,p_-s_-}\big|^2, \tag{21}$$

with

$$\big|S^{(n)}_{p_+s_+,p_-s_-}\big|^2 = \frac{Z^2}{q_+^0 q_-^0}\big|\mathfrak{M}^{(n)}_{p_+s_+,p_-s_-}\big|^2\frac{32\pi^3}{\boldsymbol{Q}_n^4}\delta\big(Q_n^0\big)cT. \tag{22}$$

Dividing out the interaction time T and multiplying by the infinitesimal phase space of the two created particles gives the partial production rate

$$d^6R_n = \frac{1}{T}\left|S^{(n)}_{p_+s_+,p_-s_-}\right|^2 \frac{d^3q_+}{(2\pi)^3}\frac{d^3q_-}{(2\pi)^3} \tag{23}$$

for any $n \geqslant n_0$ in a fully differential form.

For later use, we also give the partial rate for detecting one of the produced leptons (e.g., the positron) with a certain longitudinal spin polarization,

$$\frac{d^2R^{\mathrm{R,L}}_n}{dE_{q_+}\,d\theta_{q_+}} = \frac{Z^2}{\pi^2}\int d\Omega_{q_-}\frac{|\boldsymbol{q}^\perp_+||\boldsymbol{q}_-|}{\boldsymbol{Q}^4_n}\sum_{s_-}\left|\mathfrak{M}^{(n)}_{p_+s_{\mathrm{R,L}},p_-s_-}\right|^2, \tag{24}$$

where $\boldsymbol{q}^\perp_\pm = (q_{\pm,x},q_{\pm,y})$ denote the momentum components transversal to the laser beam direction. The positron's spin vector in Eq. (24) is chosen to be either s_{R} or s_{L}, and the matrix element is summed over the two electron spin configurations. The integration is carried out over the full solid angle of the emitted electron. The sum of $d^2R^{\mathrm{R}}_n$ ($d^2R^{\mathrm{L}}_n$) of Eq. (24) over n gives the probability rate for *measuring* a right-handed (left-handed) positron with certain energy and certain emission angle at the detector.

C. Spin-dependent matrix element $\mathfrak{M}$

The complex matrix element first occurring in Eq. (18) is defined as

$$\mathfrak{M}^{(n)}_{p_+s_+,p_-s_-} = \overline{u}_{p_-,s_-}\Gamma^{(n)}v_{p_+,s_+}\,, \tag{25}$$

with the matrix $\Gamma^{(n)}$ given by

$$\Gamma^{(n)} = \left(\not\epsilon - \frac{a^2(\epsilon k)}{2c^2(kp_+)(kp_-)}\not k\right)B_n + \left(\frac{\not\epsilon\not k\not a_1}{2c(kp_+)} - \frac{\not a_1\not k\not\epsilon}{2c(kp_-)}\right)C_n + \left(\frac{\not\epsilon\not k\not a_2}{2c(kp_+)} - \frac{\not a_2\not k\not\epsilon}{2c(kp_-)}\right)D_n\,. \tag{26}$$

The complex factors B_n, C_n, and D_n denote the Fourier expansion coefficients resulting from application of Eq. (17). They read

$$\begin{aligned} B_n &= J_n(\bar\alpha)e^{in\eta_0},\\ C_n &= \frac{1}{2}[J_{n+1}(\bar\alpha)e^{i(n+1)\eta_0} + J_{n-1}(\bar\alpha)e^{i(n-1)\eta_0}],\\ D_n &= \frac{1}{2i}[J_{n+1}(\bar\alpha)e^{i(n+1)\eta_0} - J_{n-1}(\bar\alpha)e^{i(n-1)\eta_0}], \end{aligned} \tag{27}$$

where $\bar\alpha = \sqrt{\alpha_1^2+\alpha_2^2}$ and the introduced angle η_0 is defined by $\cos\eta_0 = \alpha_1/\bar\alpha$ and $\sin\eta_0 = \alpha_2/\bar\alpha$.

We note that the matrix element (25) contains all dependencies on the laser parameters and the lepton spins. It enters into expression (24) for the production rates in terms of its squared absolute value. In index notation, we have

$$\begin{aligned} \left|\mathfrak{M}^{(n)}_{p_+s_+,p_-s_-}\right|^2 &= |\overline{u}_\alpha\Gamma^{(n)}_{\alpha\beta}v_\beta|^2 = \overline{u}_\alpha\Gamma^{(n)}_{\alpha\beta}v_\beta\overline{v}_{\beta'}\overline{\Gamma^{(n)}}_{\beta'\alpha'}u_{\alpha'}\\ &= \Gamma^{(n)}_{\alpha\beta}v_\beta\overline{v}_{\beta'}\overline{\Gamma^{(n)}}_{\beta'\alpha'}u_{\alpha'}\overline{u}_\alpha\,. \end{aligned} \tag{28}$$

The tensor products of the free Dirac spinors with themselves just equal the product of the energy projection and spin-projection operators (see [39]). Hence, Eq. (28) can be rewritten in form of a trace as

$$\left|\mathfrak{M}^{(n)}_{p_+s_+,p_-s_-}\right|^2 = \mathrm{Tr}\left\{\Gamma^{(n)}\left[\left(\frac{\not p_+ - c}{2c}\right)\left(\frac{1+\gamma^5\not s_+}{2}\right)\right]\times\overline{\Gamma^{(n)}}\left[\left(\frac{\not p_- + c}{2c}\right)\left(\frac{1+\gamma^5\not s_-}{2}\right)\right]\right\}. \tag{29}$$

This expression can be evaluated by using the standard trace technique for Dirac matrices [39]. The calculation, involving traces with up to ten Dirac matrices, is straightforward but rather tedious. The lengthy final expression shall not be given here.

However, one important property of the matrix element should be mentioned. It is symmetric under exchange of the leptons, i.e.,

$$\left|\mathfrak{M}^{(n)}_{p_+s_+,p_-s_-}\right|^2 = \left|\mathfrak{M}^{(n)}_{p_-s_-,p_+s_+}\right|^2. \tag{30}$$

As a consequence, the differential production rates of Eq. (24) and the polarization properties of the electron and the positron are identical within the present approach. This symmetry would vanish when higher orders of the Coulombic interaction were accounted for.

III. SINGLE-PHOTON PROCESS

In this section, we consider the polarization properties of a lepton beam produced via the linear Bethe-Heitler process (1), involving only a single photon of energy $\hbar\omega_\gamma > 2mc^2$. We assume that only one of the produced leptons is detected. The corresponding degree of longitudinal polarization for, say, a positron beam has first been calculated by McVoy [4] and Olsen and Maximon [5], both using a perturbative approach. The mechanisms of helicity transfer in the single-photon process have also been studied via explicit calculation of matrix elements by Pratt [42].

In the high-energy limit $\hbar\omega_\gamma \gg 2mc^2$, McVoy [4] gives the energy-dependent spin-resolved cross sections, from which the degree of longitudinal polarization, depending on the detected particle's energy E, is obtained:

$$P_\parallel(E) = \frac{d\sigma_{\mathrm{R}} - d\sigma_{\mathrm{L}}}{d\sigma_{\mathrm{R}} + d\sigma_{\mathrm{L}}} = \frac{4x-1}{4x^2-4x+3}, \tag{31}$$

where $x = E/\hbar\omega_\gamma$ denotes the fraction of the incident photon energy transmitted to the considered particle. We note that Eq. (31) has been obtained after integration by the polar emission angle of the particle. This is justified because, for high photon energies, the particles are emitted into a very narrow cone. The fundamental kinetic properties of the produced particles are exemplified in [40].

As a suitable test for the theoretical framework developed in the previous section, we have used our approach to calculate the degree of longitudinal polarization of one of the leptons produced by a 20-MeV photon impinging on a nucleus at rest. A very small value of the laser intensity parameter has been assumed ($\xi = 10^{-3}$) to make sure that the contributions from higher photon orders ($n \geqslant 2$) as well as mass shift effects [see Eq. (13)] are negligible. By dividing out the incident photon flux, we can transform the relevant pair-production rates $dR^{\mathrm{R,L}}_1$ into cross sections. Alternatively, since from the degree of longitudinal polarization $P_\parallel$ (representing a ratio

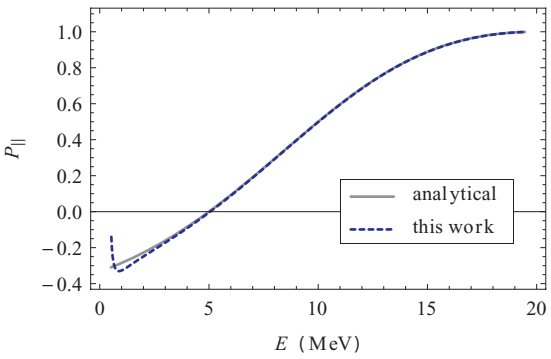

FIG. 1. (Color online) Energy-dependent degree of longitudinal polarization of a lepton beam produced via the linear Bethe-Heitler process with 20-MeV photons. The gray solid line represents the analytical result from Eq. (31), whereas the blue dashed line shows the numerical result obtained from the present approach.

of cross sections) the photon flux drops out anyway, we may express $P_\parallel$ also directly via the production rates.

Our result for the energy-dependent degree of polarization of the lepton beam is shown as the blue dashed line in Fig. 1 together with the degree of polarization predicted by Eq. (31) (solid gray line). We find overall an excellent agreement of both theories. Small deviations only arise at low lepton energies. They are due to the different approximations applied. McVoy [4] used Sommerfeld-Maue states for the derivation of Eq. (31). These are convenient for the representation of leptons moving at high velocities in a Coulomb field but are not as appropriate at small lepton energies. For low energies, our approach is even more approximate since the Volkov description of the leptons neglects interactions with the Coulomb field completely. This is the reason for the small differences visible at low lepton energies in Fig. 1. We note, however, that in case of Bethe-Heitler pair production on a proton ($Z = 1$) the influence of higher-order corrections in the Coulomb field is rather weak, rendering the present approximation reasonable. The convincing agreement of the numerical result obtained within our laser-dressed approach with the well-established result of Eq. (31) indicates that our theory is suitable for the description of polarization effects in the Bethe-Heitler process and their generalization to the multiphoton case (2).

Before proceeding to the multiphoton case, we wish to give an intuitive interpretation of the result shown in Fig. 1. The main feature is that the faster of the produced particles is more likely to be polarized in the same direction as the photon than the slower partner. It is interesting to note that this finding is not explicable in terms of angular momentum conservation, as was shown in [4]. Indeed, subtle quantum-mechanical interference cancellations between matrix elements prevent this line of argument. Instead, the following picture of helicity transfer in the high-energy limit ($\hbar\omega_\gamma \gg 2mc^2$) may be drawn. Let us assume that the photon transfers the main part of its energy to one of the particles, whereas the other one is produced almost at rest. Then the faster particle will be ultrarelativistic. Its kinematics may thus be considered as *photonlike*, in the sense that it fulfills the energy-momentum relation $E \approx |\boldsymbol{p}|c$ of a massless particle [43]. According to Fig. 1, the photonlike nature of the particle is not only restricted to its kinematical features but also comprises its polarization properties. In fact, the more energetic the produced lepton is, the more likely it will preserve the photon's helicity. Thus, in our case where photons with positive helicity are considered, the faster particle exhibits a high positive degree of longitudinal polarization.

IV. MULTIPHOTON PAIR CREATION: RESULTS FROM THE PROTON REST FRAME

Our analysis extends to the multiphoton regime where, in accordance with Eq. (2), an electron-positron pair is produced via the absorption of several photons from a laser field with $\xi \ll 1$. The question naturally arises whether the degree of longitudinal polarization can be enhanced in this case where more than one photon of the same helicity is absorbed to produce the pair. In this section we discuss the process in the rest frame of the proton where a comparison with the known results on the linear Bethe-Heitler effect can be carried out.

We note that, due to the small value of ξ in the multiphoton regime, only the process of lowest photon order n_0 typically makes a significant contribution to the total production rate. The production rate with photon order $n_0 + 1$ is suppressed by a factor of ξ^2 compared to the leading-order process. Therefore, a *genuinely* multiphoton pair-creation process requires the photon energy to be less than $2mc^2$ (in the proton rest frame) because otherwise the linear Bethe-Heitler reaction will dominate the pair production. This situation will be studied in detail in Sec. IV B. First, however, we examine in Sec. IV A a different case where the pairs are created by absorption of a few photons each having an energy larger than $2mc^2$.

We also note that in the multiphoton regime an explicit distinction between effective lepton momenta q^μ and free lepton momenta p^μ is not crucial. In the case of low-intensity parameters ($\xi \ll 1$) the relations $q^\mu \approx p^\mu$ and $m_* \approx m$ are well fulfilled [see Eqs. (13) and (14)].

A. Total photon energy of 20 MeV

In Sec. III we discussed Bethe-Heitler pair creation by a single photon of 20-MeV energy. As a direct generalization of Fig. 1, let us consider pair production by the absorption of $n = 2$, 3, or 4 laser photons which possess the same total energy (i.e., $n\hbar\omega_{\rm nuc} = 20\,{\rm MeV}$). The corresponding degrees of longitudinal polarization are shown in Fig. 2, together with the result for $n = 1$. The curves have very similar shapes and display a clear trend towards higher values of the polarization degree when the number of photons grows. Hence, under the present circumstances, multiphoton absorption can indeed enhance the degree of polarization of the produced leptons.

However, it is clear that when photons of, for example, 10 MeV energy (as in the case of $n = 2$ in Fig. 2) impinge on a proton at rest, then electron-positron pairs can already be produced by single-photon absorption. As mentioned above, the corresponding production rate R_2 for two-photon absorption will be suppressed by a factor of ξ^2 compared to the rate R_1 for the single-photon case. Hence, leptons with energies in the interval from mc^2 to $(10\,{\rm MeV} - mc^2)$ will be created predominantly by the single-photon process absorbing

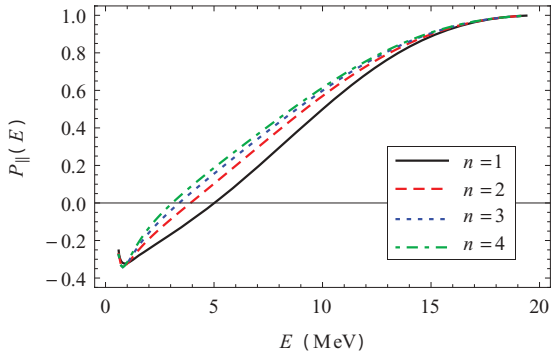

FIG. 2. (Color online) Energy-dependent degree of longitudinal polarization of one of the leptons produced via the reaction $p + n\omega \to p + e^+e^-$ for $n = 1,2,3,4$ as indicated. The total energy of the n absorbed photons is kept at the constant value of $n\hbar\omega_{\rm nuc} = 20$ MeV.

10 MeV from the laser field. At energies above 10 MeV, however, the single-photon channel is closed, and the produced leptons originate from two-photon absorption.

B. Total photon energy of 1.5 MeV

Now we turn to pair-production processes which exhibit a genuine multiphoton nature. We consider photons from a laser field with an invariant intensity parameter of $\xi = 10^{-2}$. The total amount of photon energy absorbed is assumed to be $n\hbar\omega_{\rm nuc} = 1.5$ MeV in the nuclear rest frame. The absorption of this certain amount of energy can be realized in genuine multiphoton processes involving $n_0 = 1,2$, or 3 photons. (Note that distributing 1.5 MeV equally over four photons would lead to $\hbar\omega_{\rm nuc} = 0.375$ MeV, so that three photons would be sufficient to overcome the pair-production threshold.)

Figure 3 shows the degree of longitudinal polarization for these three different processes. It is defined as the asymmetry ratio between the rates for measuring right-handed and left-handed positrons, according to

$$P_\parallel(E,\theta) = \frac{d^2R_{\rm R} - d^2R_{\rm L}}{d^2R_{\rm R} + d^2R_{\rm L}}, \tag{32}$$

where $d^2R_{\rm R/L} = d^2R^{\rm R/L}_{n_0}(E,\theta)$ is the double-differential production rate with respect to a given energy and polar angle of the particle [see Eq. (24)]. Note that, in contrast to Secs. III and IV A, an integration over the polar emission angle is not appropriate here. The particles are emitted into a rather wide angular range because their energies are not ultrarelativistic.

Figure 3 illustrates that both positive and negative degrees of longitudinal polarization are attained in all three cases. Negative degrees of polarization [red areas] are obtained in the region of low energy and orientations antiparallel to the laser direction. High positive degrees of polarization [blue areas] can be obtained both in the region of extremely small angles or in the region of energies close to the maximum.

The lepton energies and angles which provide significant contributions to the pair-production rate are determined by the matrix element in Eq. (25), in conjunction with obvious kinematic restrictions imposed by energy conservation. The contours in Fig. 3 are drawn equidistantly in the interval from

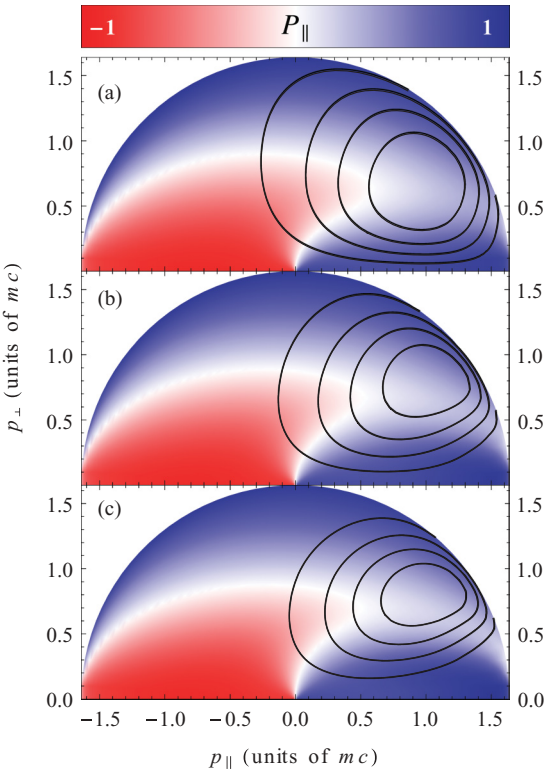

FIG. 3. (Color online) Color-coded degree of longitudinal polarization for the absorption of (a) one, (b) two and (c) three photons with a total energy of $n\hbar\omega_{\rm nuc} = 1.5$ MeV as a function of the transversal and parallel momentum components of the lepton with respect to the laser beam. Negative degrees of polarization [red areas in the lower left of each panel] occur at large emission angles in the proton rest frame, while positive degrees of polarization [blue areas] arise at high energies and at small angles. Contours of the double-differential production rates are plotted as black lines at every fifth part of the corresponding maximum value [see Eqs. (33)–(35)].

zero to the maximum value of the double-differential rate. In the case of Fig. 3(a), the maximum occurs at the peak values $\hat{E} \approx 1.55mc^2$ and $\hat{\theta} \approx 0.19\pi$ and amounts to

$$\left.\frac{d^2R^{\rm R+L}_{n_0=1}}{dE\,d\theta}\right|_{\rm max} \approx 8.3\times10^{10}\,\frac{\rm s^{-1}}{(mc^2){\rm rad}}. \tag{33}$$

We can therefore conclude that the produced positron beam has, on average, a moderately positive degree of polarization of $P_\parallel \sim 1/4$.

By considering laser photons with only half the energy as before ($\hbar\omega_{\rm nuc} = 0.75$ MeV), the production channel corresponding to the absorption of only one photon is closed, and the most favorable process of lowest possible photon order takes place at $n_0 = 2$. Figure 3(b) shows the same quantities as Fig. 3(a), but for the two-photon case. The maximum of the double-differential rate is

$$\left.\frac{d^2R^{\rm R+L}_{n_0=2}}{dE\,d\theta}\right|_{\rm max} \approx 2.1\times10^{6}\,\frac{\rm s^{-1}}{(mc^2){\rm rad}}. \tag{34}$$

It is located at $\hat{E} \approx 1.7mc^2$ and $\hat{\theta} \approx 0.2\pi$. Compared to the one-photon process involving a laser photon with twice the energy, the distribution of angles has become narrower, and

the energy distribution has shifted to higher values (see also [34]). Nevertheless, the main part of the positrons is still produced in a region where no significantly high degrees of polarization are achieved. Most of the particles are again produced with positive but low degrees of polarization ($P_\parallel \sim 1/4$).

Taking the photon energy in the proton rest frame to be $\hbar\omega_{\rm nuc} = 0.5\,\text{MeV}$ ensures that both the processes involving one and two photons are kinematically forbidden. The leading photon order is $n_0 = 3$ in this case. Figure 3(c) shows the degree of longitudinal polarization depending on the positron momentum components. The distribution of the production rate in momentum space has slightly narrowed. The maximum production rate is

$$\left.\frac{d^2R^{\rm R+L}_{n_0=3}}{dE\,d\theta}\right|_{\rm max} \approx 88\frac{\rm s^{-1}}{(mc^2)\rm rad} \tag{35}$$

at a peak energy of $\hat{E} \approx 1.65mc^2$ and a peak angle of $\hat{\theta} \approx 0.22\pi$. Even when absorbing three photons all carrying the same helicity, the distribution of polarization does not change significantly. Only moderate degrees of longitudinal polarization can be achieved with non-negligible probability. This circumstance promotes the concept of strong coupling between helicity transfer and energy transfer.

To give more quantitative results, Fig. 4 presents the double-differential rates $d^2R_{n_0}$ as a function of the lepton energy E at a fixed angle θ for all the three processes. The spin-resolved rates $d^2R^{\rm R/L}_{n_0}$ are shown, together with the total (i.e., spin-summed) rate $d^2R^{\rm R+L}_{n_0}$. In each case, the peak value $\hat{\theta}$ has been chosen for the angle, and the rates have been scaled with their corresponding maximum values [see Eqs. (33)–(35)]. We find that the shape of the total production rates (black lines) for the different photon orders shifts only slightly toward higher energies for increasing photon order. However, it can clearly be seen that right-handed particles are more likely to be detected with higher energies (cf. blue dashed lines), while the mean energy of left-handed particles lies below the corresponding value of $\hat{E}$ (cf. red dotted lines).

From Fig. 4 one can extract the corresponding degrees of longitudinal polarization, which are shown in Fig. 5. While the polarization degree is positive everywhere, sizable values of $P_\parallel \approx 0.7$ are reached only around the minimum and maximum lepton energies. In these regions, however, the underlying production rates are very small. In the region around $E \approx \hat{E}$, where the production rates are largest, only small degrees of polarization are reached, $P_\parallel \approx 0.25$. As a comparison, we note that for the parameters of Fig. 1 the production rate is largest around $E \approx 10$ MeV (where the leptons share the photon energy in approximately equal amounts); the corresponding degree of longitudinal polarization is substantial and amounts to $P_\parallel \approx 0.5$.

The smaller degrees of longitudinal polarization found for the parameters of Fig. 5 as compared with Fig. 1 may be attributed to the largely different energies which the leptons have in each case. While in the situation of Fig. 1, the typical lepton energy is ultrarelativistic, the lepton kinematics is only weakly relativistic in Fig. 5. In fact, for a genuinely multiphoton process with $n_0 > 1$, the maximum kinetic energy

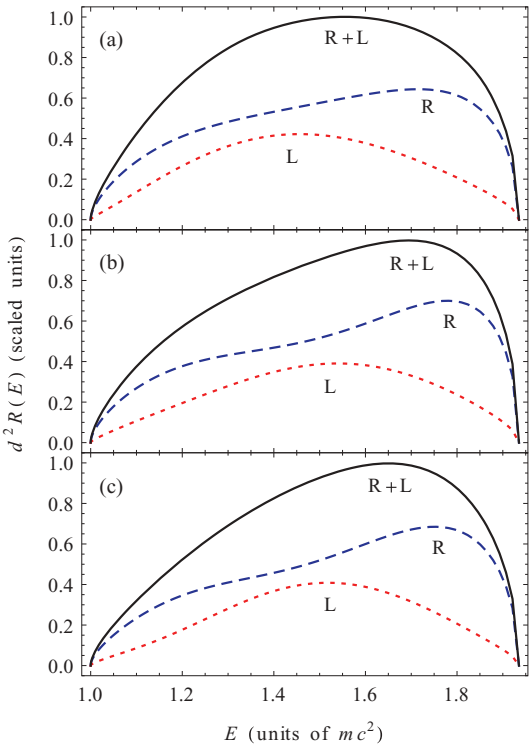

FIG. 4. (Color online) Double-differential rates at fixed angle $\hat{\theta}$ plotted against the created lepton's energy in the proton's rest frame for the absorption of (a) one, (b) two, and (c) three photons with a total energy of $n\hbar\omega_{\rm nuc} = 1.5$ MeV. Each graph shows the total spin-summed rate (black solid line) together with the corresponding probability rates for measuring a right-handed (blue dashed line) or left-handed (red dotted line) lepton in the proton's rest frame. The rates are scaled to their corresponding maximum values [see Eqs. (33)–(35)].

of one of the leptons is given by

$$E^{\rm max}_{\rm kin} = n_0\hbar\omega^{\rm max}_{\rm nuc} - 2mc^2 = \frac{2mc^2}{n_0 - 1}\,. \tag{36}$$

Here, $\hbar\omega^{\rm max}_{\rm nuc}$ is the maximum photon energy which allows multiphoton pair production with the leading photon order being n_0. For higher photon energies, a lower-order process

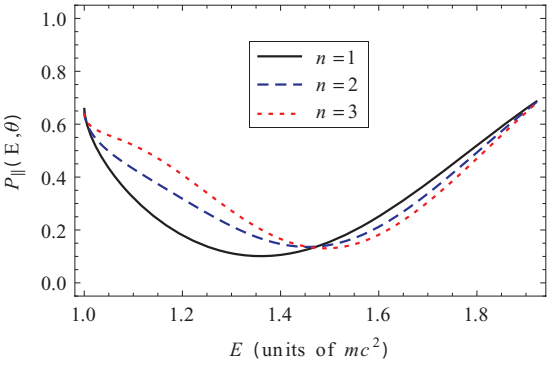

FIG. 5. (Color online) Degree of longitudinal polarization at fixed angle $\theta = \pi/5$ plotted against the created lepton's energy in the proton's rest frame for the absorption of $n = 1,2$, or 3 photons, as indicated. The total photon energy is $n\hbar\omega_{\rm nuc} = 1.5$ MeV.

will be the most favorable $[n_0 \to (n_0 - 1)]$. According to Eq. (36), the energies of the leptons produced in a genuinely multiphoton process cannot be highly relativistic. Thus, none of the produced particles may be considered as photonlike. Our intuitive picture of helicity transfer developed in Sec. III therefore suggests that leptons generated through a genuinely multiphoton process cannot attain degrees of polarization as high as in the high-energy single-photon case.

V. MULTIPHOTON PAIR CREATION: RESULTS FROM THE LABORATORY FRAME

In the previous section we discussed the polarization properties of the leptons in the nuclear rest frame. These results are mainly of theoretical interest since the particles can naturally be considered to be produced in that frame. In the following, we analyze the lepton polarization in the laboratory frame where the nucleus is moving with high Lorentz factor γ and high velocity $v = \beta c$. This is the frame where an experimental measurement would actually be carried out.

The helicity of massive particles is not a Lorentz invariant quantity. Therefore, in order to study the longitudinal polarization in the laboratory frame, the spin vectors have to be determined with respect to the momentum vectors in this frame. Both the momentum vectors and the spin vectors may then be Lorentz transformed to the nucleus' rest frame, where the production rates are evaluated. We recall that our theoretical framework in Sec. II can be applied to any spin basis.

The spin vectors entering the matrix element (29) are related to the four-momentum $p^\mu = (E/c, \boldsymbol{p}_\perp, p_\parallel)$ in the proton frame via

$$s^\mu_{\mathrm{R,L}} = \pm \frac{\gamma}{mc} \frac{1}{\sqrt{\boldsymbol{p}_\perp^2 + \left(p_\parallel - \beta\gamma \frac{E}{c}\right)^2}} \tilde{s}^\mu, \tag{37}$$

with the newly defined four-component vector $\tilde{s}^\mu$ given by

$$\begin{aligned} \tilde{s}^0 &= \boldsymbol{p}_\perp^2 + p_\parallel \left(p_\parallel - \beta \frac{E}{c}\right), \\ \tilde{\boldsymbol{s}}_\perp &= \left(\frac{E}{c} - \beta p_\parallel\right) \boldsymbol{p}_\perp, \\ \tilde{s}_\parallel &= \beta \boldsymbol{p}_\perp^2 + \frac{E}{c}\left(p_\parallel - \beta \frac{E}{c}\right). \end{aligned} \tag{38}$$

The spatial coordinates have been split up into their components parallel and transversal to the z direction. When the spin vectors (37) are transformed back to the laboratory frame, they will be parallel (or antiparallel) to the momentum vectors of the leptons in this frame. Hence, the transformation of the spin-resolved production rates calculated in the nucleus' frame with the spin vectors (37) gives helicity-resolved production rates in the laboratory frame.

We consider nonlinear Bethe-Heitler pair production in a situation where the Lorentz factor of the proton is $\gamma = 100$ and a total photon energy of $n\hbar\omega_{\mathrm{lab}} = 7.5$ keV is absorbed ($n = 1,2,3$). Accordingly, in the proton frame, the absorbed photon energy amounts to 1.5 MeV as in Figs. 3–5. The optimum values $(\hat{E}, \hat{\theta})$ given in Sec. IV B are denoted by $(\hat{E}_{\mathrm{lab}}, \hat{\theta}_{\mathrm{lab}})$ after Lorentz transformation to the laboratory frame.

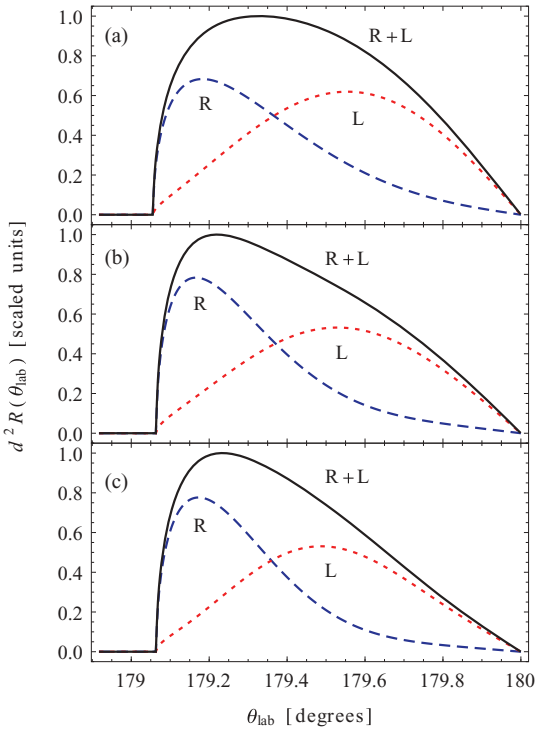

FIG. 6. (Color online) Double-differential pair-production rates in the laboratory frame at a fixed lepton energy $\hat{E}_{\mathrm{lab}}$, plotted against the lepton emission angle with respect to the laser beam direction for the absorption of (a) one, (b) two, and (c) three photons with a total energy of $n\hbar\omega_{\mathrm{lab}} = 7.5$ keV. The photons collide with a proton beam of 94-GeV energy ($\gamma = 100$). Each graph shows the total spin-summed rate (black solid line) together with the corresponding probability rates for measuring a right-handed (blue dashed line) or left-handed (red dotted line) lepton in the laboratory frame. The rates are scaled to their corresponding maximum values.

Results for double-differential production rates in the laboratory frame are presented in Fig. 6. They have been scaled to their respective maximum values and are plotted against the polar angle θ_{lab} at the fixed energy $\hat{E}_{\mathrm{lab}} \approx 60mc^2$, for $n_0 = 1,2,3$. We find that the cone into which the leptons are emitted is very narrow, $\theta_{\mathrm{lab}} > 179^\circ$. This is due to the large amount of momentum carried by the relativistic proton, in comparison to the negligible amount of momentum carried by the laser photons in the laboratory frame. We further observe that right-handed leptons are preferably emitted under slightly smaller angles than left-handed leptons, which is a consequence of the Lorentz-transformation-induced inversion of the cone in which the particles are produced. This means that in the inner region of the lepton beam that travels essentially in the direction of the nuclear beam the particles are more likely to be found in a left-handed state, while in the outer region of the beam the leptons are preferably detected in right-handed states.

Figure 7 shows the degree of longitudinal polarization in the laboratory frame as a function of the lepton energy. Since the leptons are emitted into a very narrow angular range, an integration over this angle has been performed (see also Figs. 1 and 2). In fact, all leptons are moving approximately along the proton beam direction so that the degree of longitudinal polarization essentially refers to this direction. One can see

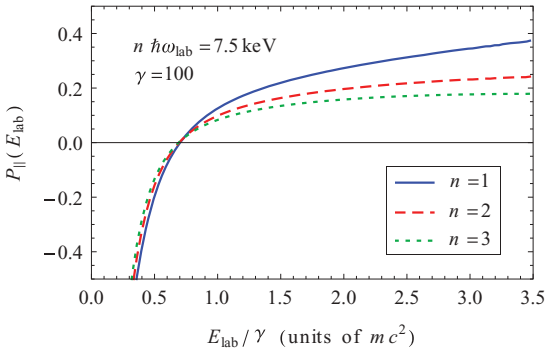

FIG. 7. (Color online) The degree of longitudinal polarization is shown for a total amount of energy $n\hbar\omega_{\rm nuc} = 1.5$ MeV at an invariant intensity parameter of $\xi = 10^{-2}$ for all possible different leading orders with the same combined energy, i.e., $n = 1,2,3$. The proton is moving at a velocity of $\gamma = 100$.

in Fig. 7 that in the energy range around $\hat{E}_{\rm lab} \approx 0.6\gamma mc^2$, where the majority of particles are actually produced, the degree of longitudinal polarization is very small but negative and is zero at $E_{\rm lab} \approx 0.7\gamma mc^2$ for all the considered photon orders. In the limit of high energies, the degree of longitudinal polarization is largest for the process with $n_0 = 1$. However, there are essentially no leptons produced at energies far above $2\gamma mc^2$.

We conclude this section by pointing out a general feature of the degree of longitudinal polarization in the laboratory frame. According to relation (36), the lepton energies and momenta in the proton frame are (at most) weakly relativistic. By Eqs. (37) and (38), this implies that already for moderate values of the nuclear Lorentz factor, $\gamma \gtrsim 10$, the spin vectors in this frame will essentially become independent of γ. Therefore, as long as the photon energy in the proton frame remains constant (which can be achieved by varying the laboratory-frame laser frequency in accordance with the change of γ), we may expect that, for sufficiently high proton energies, the degree of longitudinal polarization only depends on the ratio $E_{\rm lab}/\gamma$, that is, $P_{\parallel} = P_{\parallel}(E_{\rm lab}/\gamma)$. This scaling behavior has been verified by numerical calculations for γ values up to 1000 at $n_0\hbar\omega_{\rm nuc} = 1.5$ MeV ($n_0 = 1,2,3$). The functional character of $P_{\parallel}(E_{\rm lab}/\gamma)$ was indeed found to be practically indistinguishable from the result shown in Fig. 7.

VI. CONCLUSION

We investigated the longitudinal spin polarization of the electron and positron produced via multiphoton absorption in the collision of a relativistic nucleus with a high-intensity laser beam of circular polarization. Our treatment combined the established laser-dressed approach to nonlinear Bethe-Heitler pair production using relativistic Volkov states with the spin-projection formalism. In contrast to previous studies, the multiphoton regime of the process was considered where the laser frequency is very high whereas the laser intensity is relatively low.

First, we investigated the transfer of helicity from the photons to the leptons in the nuclear rest frame. The well-known result for the degree of longitudinal polarization obtained in the ordinary Bethe-Heitler process involving a single high-energy photon has been reproduced, and an intuitive explanation of its main characteristics has been offered. Then, we showed that the degree of longitudinal polarization is increased when the pairs are produced by absorption of several photons with the same total energy such that $n\hbar\omega_{\rm nuc} \gg 2mc^2$. In a genuinely multiphoton process where $n\hbar\omega_{\rm nuc} \gtrsim 2mc^2$, the polarization of the leptons also exhibits a dependence on the number of laser photons absorbed, but the achievable degrees of polarization are substantially reduced. From these results we may conclude that the efficiency of helicity transfer depends on an interplay between the number of photons involved and the total photon energy absorbed, with the latter parameter being more relevant. In view of practical purposes of producing electron and positron beams with a high degree of longitudinal polarization, our study has shown that the established procedure of exploiting the linear Bethe-Heitler effect (1) with a single high-energy photon is more effective than utilizing its nonlinear generalization (2) due to the lack of high-energy transfer in a genuinely multiphoton process.

In the laboratory frame, where the nucleus is moving at high speed, we have found that leptons with the same helicity as the laser photons are more likely to be detected under larger angles with respect to the proton beam than those of opposite helicity. This feature has also been obtained in the tunneling regime of nonlinear Bethe-Heitler pair production [37]. In addition, the degree of longitudinal polarization in the laboratory frame was shown to become independent of the proton Lorentz factor at sufficiently high proton energies, provided that the laser photon energy in the proton rest frame remains constant.

Our results could, in principle, be probed in an experimental facility which combines an intense laser beam of circular polarization with a powerful ion accelerator. The required laser photon energies of the order of mc^2 in the nuclear rest frame can be achieved when (i) an intense xuv laser source ($\hbar\omega_L \sim 20$–70 eV, $I_L \sim 10^{17}$ W/cm^2, $\xi \sim 10^{-2}$) is operated at the proton beam line of the Large Hadron Collider at CERN ($\gamma \sim 3000$–7000) or (ii) a high-intensity x-ray laser facility ($\hbar\omega_L \sim 10$ keV, $I_L \sim 10^{22}$ W/cm^2, $\xi \sim 10^{-2}$) could be combined with an ion accelerator providing Lorentz factors of $\gamma \sim 25$–75. We note that proton beams of the corresponding energy might also become available via violent laser acceleration [44]. For comparison we briefly comment on the present status of high-intensity xuv and x-ray laser sources. The free-electron laser-based FLASH facility (DESY, Germany) generates brilliant photon beams with xuv photon energies of $\hbar\omega_L \sim 100$ eV and intensities up to $\sim 10^{17}$ W/cm^2 [45]. The free-electron laser at the Linac Coherent Light Source (SLAC, Stanford) is currently able to produce x-ray beams with $\hbar\omega_L \sim 1$ keV at peak intensities of $\sim 10^{18}$ W/cm^2 [46]. A considerable further increase of the achievable photon intensities is envisaged at both laboratories. Intense coherent xuv and x-ray pulses are also attainable by high-harmonic emission from laser-irradiated plasma surfaces [47].

ACKNOWLEDGMENT

Useful discussions with A. I. Milstein are gratefully acknowledged.

[1] T. D. Lee and C. N. Yang, Phys. Rev. **104**, 254 (1956).
[2] U. Fano, Phys. Rev. **178**, 131 (1969).
[3] S. C. Miller and R. M. Wilcox, Phys. Rev. **124**, 637 (1961).
[4] K. W. McVoy, Phys. Rev. **106**, 828 (1957); K. W. McVoy and F. J. Dyson, *ibid.* **106**, 1360 (1957); K. W. McVoy, *ibid.* **111**, 1333 (1958).
[5] H. Olsen and L. C. Maximon, Phys. Rev. **110**, 589 (1958); **114**, 887 (1959).
[6] T. Omori *et al.*, Phys. Rev. Lett. **96**, 114801 (2006).
[7] G. Alexander *et al.*, Phys. Rev. Lett. **100**, 210801 (2008).
[8] D. B. Milošević and F. Ehlotzky, Adv. At. Mol. Opt. Phys. **49**, 373 (2003).
[9] D. B. Milošević, G. G. Paulus, D. Bauer, and W. Becker, J. Phys. B **39**, R203 (2006).
[10] Y. I. Salamin, S. X. Hu, K. Z. Hatsagortsyan, and C. H. Keitel, Phys. Rep. **427**, 41 (2006).
[11] F. Ehlotzky, K. Krajewska, and J. Z. Kamiński, Rep. Prog. Phys. **72**, 046401 (2009).
[12] M. W. Walser, D. J. Urbach, K. Z. Hatsagortsyan, S. X. Hu, and C. H. Keitel, Phys. Rev. A **65**, 043410 (2002).
[13] J. San Roman, L. Roso, and L. Plaja, J. Phys. B **36**, 2253 (2003).
[14] F. H. M. Faisal and S. Bhattacharyya, Phys. Rev. Lett. **93**, 053002 (2004).
[15] S. Bhattacharyya, M. Mukherjee, M. Mazumder, and F. H. M. Faisal, Phys. Rev. A **80**, 013418 (2009).
[16] M. Walser and C. Keitel, Opt. Commun. **199**, 447 (2001).
[17] D. Y. Ivanov, G. L. Kotkin, and V. G. Serbo, Eur. Phys. J. C **36**, 127 (2004).
[18] C. Szymanowski, R. Taïeb, and A. Maquet, Laser Phys. **8**, 102 (1998).
[19] P. Panek, J. Z. Kamiński, and F. Ehlotzky, Phys. Rev. A **65**, 033408 (2002).
[20] Y. S. Tsai, Phys. Rev. D **48**, 96 (1993).
[21] D. Y. Ivanov, G. L. Kotkin, and V. G. Serbo, Eur. Phys. J. C **40**, 27 (2005).
[22] V. S. Popov, Sov. JETP **34**, 709 (1972).
[23] P. Krekora, Q. Su, and R. Grobe, Phys. Rev. Lett. **92**, 040406 (2004); R. E. Wagner, M. R. Ware, Q. Su, and R. Grobe, Phys. Rev. A **81**, 024101 (2010).
[24] D. Burke *et al.*, Phys. Rev. Lett. **79**, 1626 (1997).
[25] V. Yakovlev, Sov. Phys. JETP **22**, 223 (1965).
[26] C. Müller, A. B. Voitkiv, and N. Grün, Phys. Rev. A **67**, 063407 (2003); **70**, 023412 (2004).
[27] P. Sieczka, K. Krajewska, J. Z. Kaminski, P. Panek, and F. Ehlotzky, Phys. Rev. A **73**, 053409 (2006).
[28] A. I. Milstein, C. Müller, K. Z. Hatsagortsyan, U. D. Jentschura, and C. H. Keitel, Phys. Rev. A **73**, 062106 (2006).
[29] M. Y. Kuchiev and D. J. Robinson, Phys. Rev. A **76**, 012107 (2007).
[30] E. Lötstedt, U. D. Jentschura, and C. H. Keitel, Phys. Rev. Lett. **101**, 203001 (2008).
[31] C. Müller, Phys. Lett. B **672**, 56 (2009).
[32] A. Di Piazza, E. Lötstedt, A. I. Milstein, and C. H. Keitel, Phys. Rev. A **81**, 062122 (2010).
[33] C. Müller, A. B. Voitkiv, and N. Grün, Phys. Rev. Lett. **91**, 223601 (2003).
[34] S. J. Müller and C. Müller, Phys. Rev. D **80**, 053014 (2009).
[35] K. Krajewska and J. Z. Kamiński, Phys. Rev. A **84**, 033416 (2011).
[36] K. Krajewska and J. Z. Kamiński, Phys. Rev. A **85**, 043404 (2012).
[37] T.-O. Müller and C. Müller, Phys. Lett. B **696**, 201 (2011).
[38] A. Di Piazza, A. I. Milstein, and C. Müller, Phys. Rev. A **82**, 062110 (2010).
[39] J. D. Bjorken and S. D. Drell, *Relativistische Quantenmechanik*, BI-Hochschultaschenbücher Vol. 98 (Bibliographisches Institut, Mannheim, Vienna, Zurich, 1984).
[40] V. B. Beresteckij, E. M. Lifšic, and L. P. Pitaevskij, *Quantenelektrodynamik* (Akademie-Verlag, Berlin, 1986).
[41] M. Abramowitz and I. A. Stegun, *Handbook of Mathematical Functions* (Dover, New York, 1965).
[42] R. H. Pratt, Phys. Rev. **123**, 1508 (1961).
[43] A. B. Voitkiv (private communication).
[44] T. Esirkepov, M. Borghesi, S. V. Bulanov, G. Mourou, and T. Tajima, Phys. Rev. Lett. **92**, 175003 (2004).
[45] W. Ackermann *et al.*, Nat. Photonics **1**, 336 (2007).
[46] L. Young *et al.*, Nature (London) **466**, 56 (2010).
[47] B. Dromey *et al.*, Nat. Phys. **5**, 146 (2009).